Appendix

PP4-dependent HDAC3 dephosphorylation discriminates between axonal regeneration and regenerative failure

Arnau Hervera[1,2§], Luming Zhou[3,4§], Ilaria Palmisano[1], Eilidh McLachlan[1], Guiping Kong[3], Thomas Hutson[1], Matt C Danzi[5], Vance P. Lemmon[5], John L. Bixby[5], Andreu Matamoros-Angles[2], Kirsi Forsberg[3], Francesco De Virgiliis[1,3,4], Dina P. Matheos[6], Janine Kwapis[6], Marcelo A. Wood[6], Radhika Puttagunta[3], José Antonio del Río[2], Simone Di Giovanni[1,3]*.

[1]Molecular Neuroregeneration, Division of Brain Sciences, Department of Medicine, Imperial College London, London, UK. [2]Molecular and Cellular Neurobiotechnology, Institute for Bioengineering of Catalonia (IBEC), Parc Científic de Barcelona, Barcelona, Spain. Centro de Investigación Biomédica en Red sobre Enfermedades Neurodegenerativas (CIBERNED), Barcelona, Spain. Department of Cell Biology, Physiology and Immunology, Universitat de Barcelona, Barcelona, Spain. Institute of Neuroscience, University of Barcelona, Barcelona. Spain. [3]Laboratory for NeuroRegeneration and Repair, Center for Neurology, Hertie Institute for Clinical Brain Research, University of Tuebingen, Tuebingen, Germany. [4]Graduate School for Cellular and Molecular Neuroscience, University of Tuebingen, Tuebingen, Germany.[5]The Miami Project to Cure Paralysis, Department of Neurological Surgery, Miller School of Medicine, University of Miami, 1400 NW 12th Ave, Miami, FL 33136, USA.

[6]Center for the Neurobiology of Learning & Memory, Dept. of Neurobiology & Behavior, University of California, Irvine, USA. [§]These authors contributed equally. To whom correspondence should be addressed.*

Table of Content

Appendix Fig 1

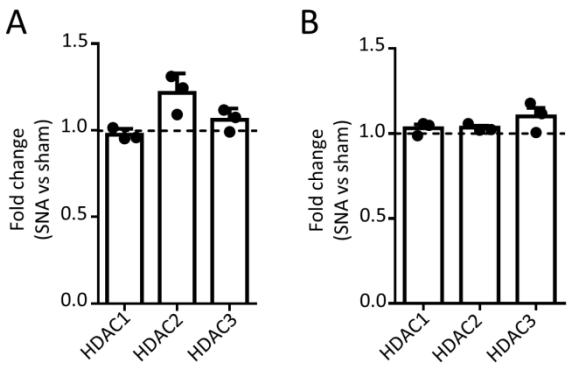

Appendix Figure S1. **Gene expression of class I HDACs in DRGs after peripheral and central axonal injuries.**

A-B. Quantitative RT-PCR showing gene expression levels of HDAC1, 2 and 3 after SNA (A) or DCA (B) vs respective sham or laminectomy. Data is expressed as mean relative expression vs sham or lam ± s.e.m. N= 3 biological replicates (ANOVA followed by Bonferroni test).

Appendix Fig 2

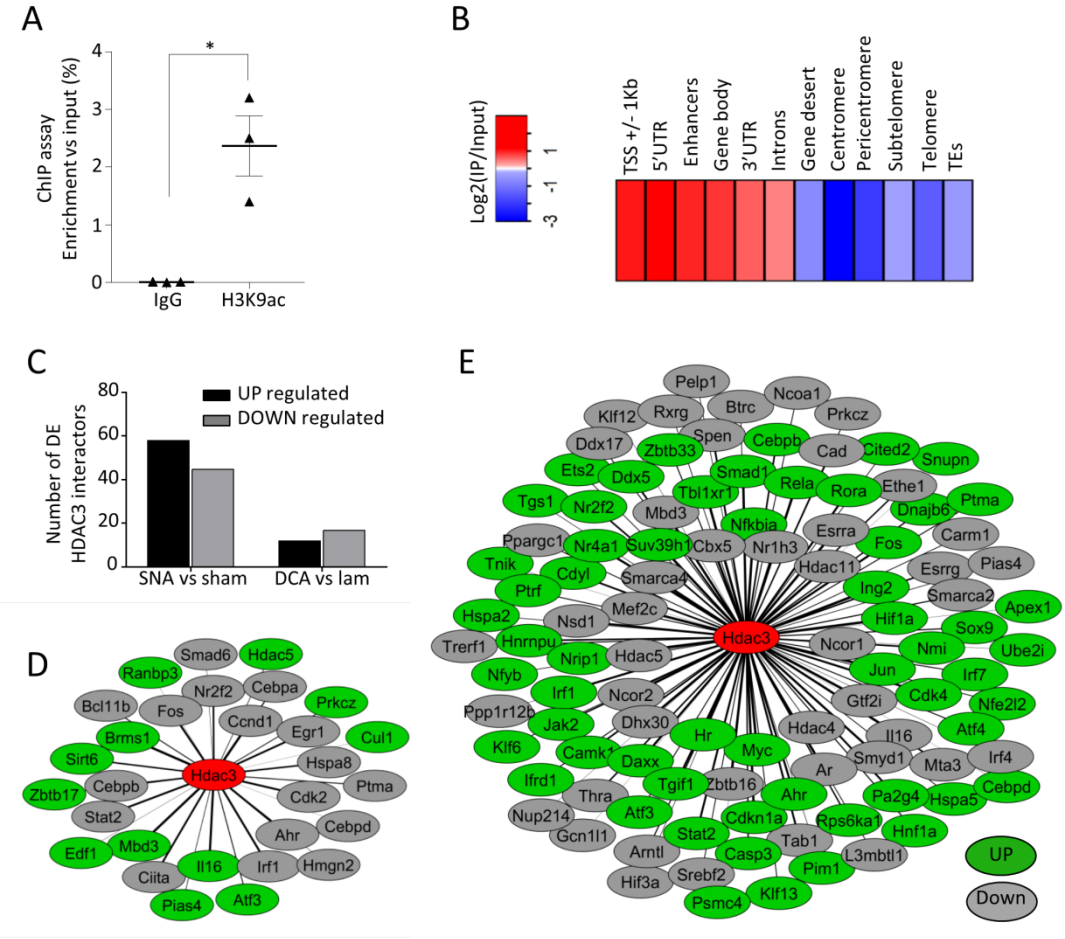

Appendix Figure S2. **H3K9ac ChIPseq and HDAC3 interactome.**

A. Assessment of the enrichment of recovered DNA after H3K9ac ChIP versus control IgG ChIP. Data is expressed as percentage with respect to Input (average ± s.e.m. of 3 independent experiments, paired Student t-test, *p<0.05). B. Heatmap showing genomic distribution of H3K9ac reads, as Log_2(IP vs Input) in a representative control sample. Note preferentially enrichment at TSS, enhancers and gene bodies. C. Bar graph shows the number of HDAC3 interactors identified using FpClass (score ≥0.4) that are differentially expressed under the indicated conditions. Note that after SNA a higher percentage of HDAC3 interactors is differentially regulated with respect to DCA. D, E. Cytoscape visualization of the HDAC3 interactors that are differentially expressed upon DCA (D) or SNA (E). Upregulated interactors are in green, downregulated are in grey, HDAC3 is in red at the center of the network. The line thickness is proportional to the interaction score.

Appendix Fig 3

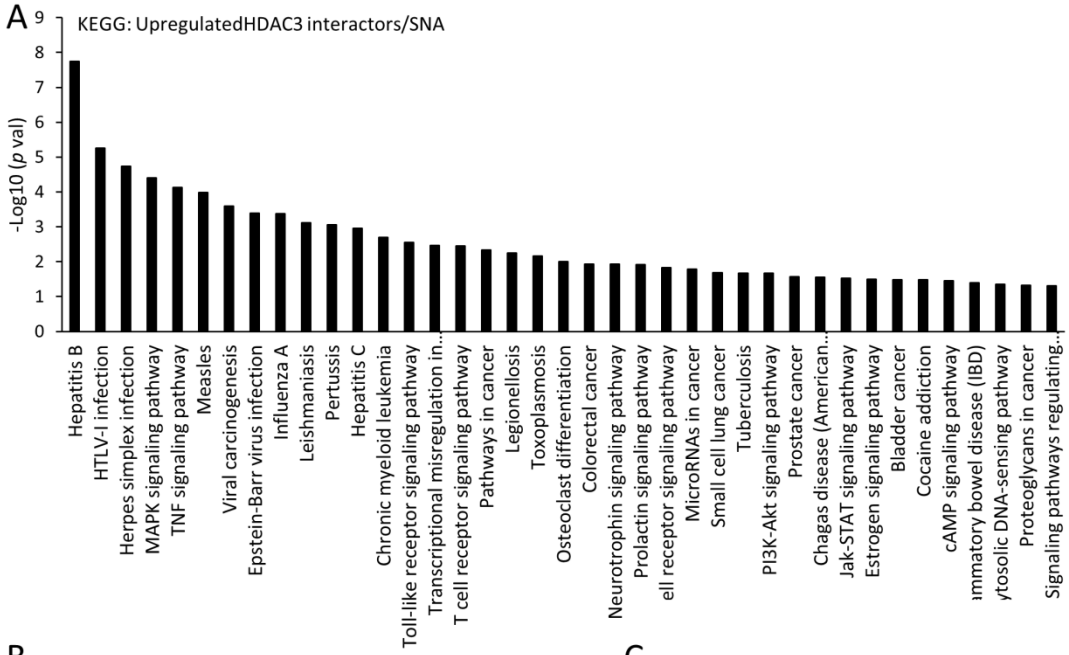

D

TF_NAME- top 17	*p*_value	Regeneration/plasticity
E2F4	6.23E-29	yes (Sasagawa et al., 2016)
SP1	6.06E-27	yes (Kiryu-Seo., 2008)
EGR1	5.15E-26	yes (Knapska et al., 2004)
E2F3	7.95E-25	
KLF5	9.09E-25	yes, inhibitor (Ribas et al., 2017)
E2F1	2.00E-24	yes (Christie et al., 2014)
KLF4	1.46E-23	yes, inhibitor (Moore et al., 2009)
TFAP2A	7.75E-21	
SP3	1.63E-20	
ZBTB33	5.00E-16	
CREB1	2.25E-14	yes (Gao et al., 2004)
KLF12	4.22E-14	yes, inhibitor (Ribas et al., 2017)
MYC	3.35E-10	yes (Belin et al., 2015)
ARNT:HIF1A	9.60E-10	yes (Cho et., 2015)
NFKB1	3.13E-09	yes, dual (Haenold et al., 2014)
ELK1	9.69E-09	yes, Lavaur et al., 2007 and Mar et al., 2014
KLF13	1.97E-08	yes, inhibitor (Ribas et al., 2017)

Appendix Figure S3. **Upregulated HDAC3 interactors are related to regenerative signalling pathways.** A. and B. Bar graph shows the KEGG pathway categories of the HDAC3 interactors sorted by -$\log_{10}$(*p* value) (cut off applied: $p<0.05$) that are up (A) or down (B) regulated after SNA.

C. Venn diagram shows common transcription factors (TF) predicted to interact with HDAC3 (HDAC3 interactors) identified after *in silico* motif enrichment analysis of upregulated genes associated with increased H3K9ac after SNA following RNAseq (75 TF total) (see supplementary methods for details). D. Table shows a list of the identified TF predicted to interact with HDAC3, sorted by *p* value, and their previous involvement in regeneration/plasticity after axonal injury.

Appendix Fig 4

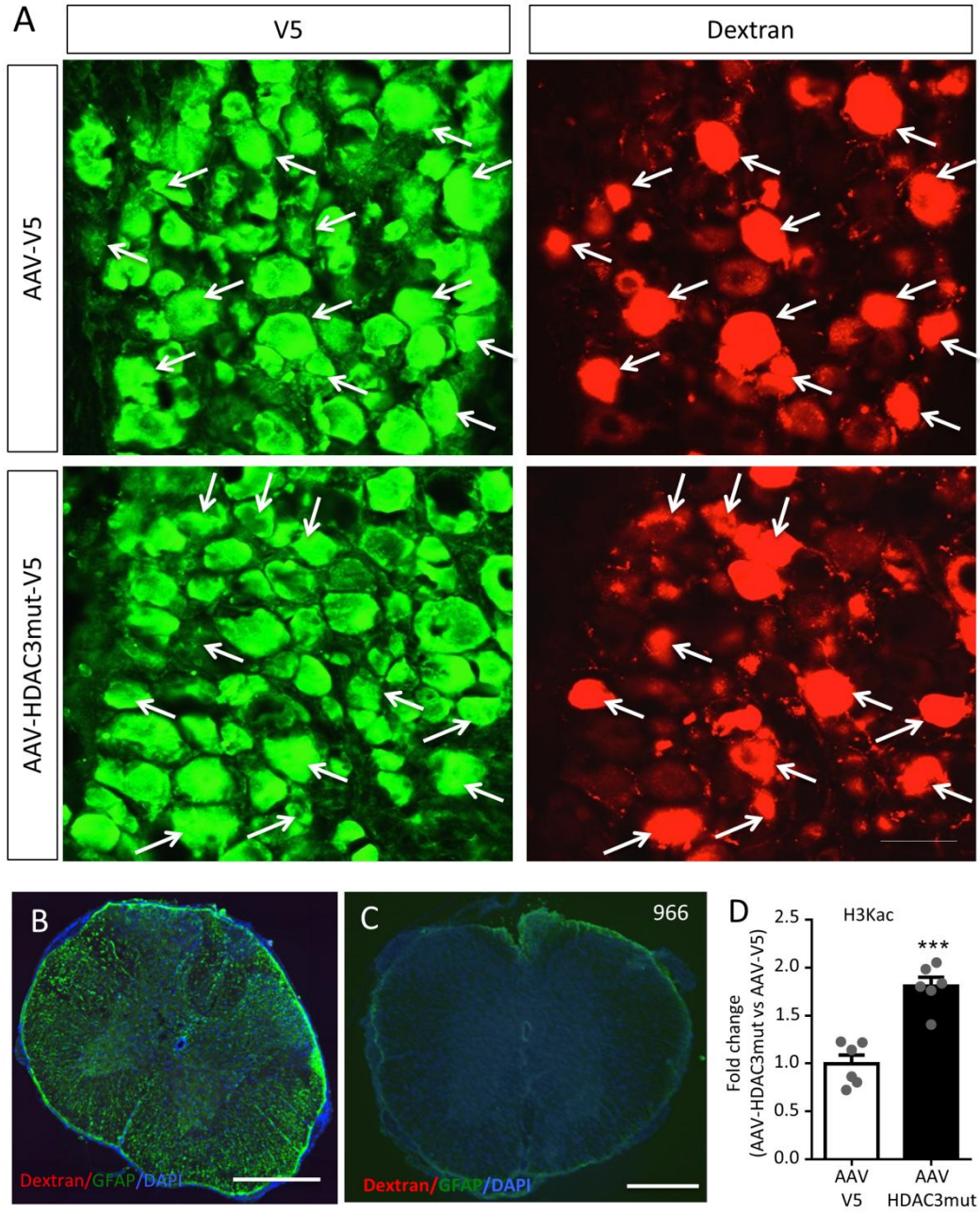

Appendix Figure S4. **Genetic inactivation of HDAC3 deacetylase activity increases H3K9ac in DRGs.** A. Immunofluorescence anti-V5 and dextran-red staining in whole DRG after sciatic nerve injection of AAV and dextran. Scale bar, 50µm. Arrows show co-localisation of V5-positive neurons in the majority of dextran-positive cells**.** B-C. Immunofluorescence anti-GFAP with fluorescent dextran and DAPI signal shows spinal cord coronal section of AAV-HDAC3 dead mutant (B) or 966 (C) treated mice 10 mm rostral from the lesion core, showing the absence of spared dextran^{+} axons. Scale bar, 500 µm D. Bar graph shows fold change of immunofluorescence intensity of H3K9ac in DRG after AAV-HDAC3mut vs control AAV± s.e.m. N= 6 animals per condition. (***$p<0.005$) indicate significant difference versus control AAV (Student's t-test).